Journal of Environmental Management 366 (2024) 121811

Contents lists available at ScienceDirect

Journal of Environmental Management

journal homepage: www.elsevier.com/locate/jenvman

Research article

Optimization of methane gas-liquid mass transfer during biogas-based ectoine production in bubble column bioreactors

María del Rosario Rodero [a,b], Víctor Pérez [a,b], Raúl Muñoz [a,b,*]

[a] Institute of Sustainable Processes, University of Valladolid, 47011, Valladolid, Spain
[b] Department of Chemical Engineering and Environmental Technology, School of Industrial Engineering. University of Valladolid, Dr. Mergelina s/n., 47011, Valladolid, Spain

ARTICLE INFO

Keywords:
Biogas valorization
Diffuser pore size
Empty bed residence time
Methanotrophs

ABSTRACT

Nowadays, the utilization of biogas for energy generation is hindered by the declining production costs of solar and wind power. A shift towards the valorization of biogas into ectoine, a highly valuable bioproduct priced at 1000 €·kg^{-1}, offers a novel approach to fostering a more competitive biogas market while contributing to carbon neutrality. This study evaluated the optimization of CH_4 gas-liquid mass transfer in 10 L bubble column bioreactors for CH_4 conversion into ectoine and hydroxyectoine using a mixed methanotrophic culture. The influence of the empty bed residence time (EBRTs of 27, 54, and 104 min) at different membrane diffuser pore sizes (0.3 and 0.6 mm) was investigated. Despite achieving CH_4 elimination capacities (CH_4-ECs) of 10–12 g·m^{-3}·h^{-1}, an EBRT of 104 min mediated CH_4 limitation within the cultivation broth, resulting in a negligible biomass growth. Reducing the EBRT to 54 min entailed CH_4-ECs of 21–24 g·m^{-3}·h^{-1}, concomitant to a significant increase in biomass growth (up to 0.17 g·L·d^{-1}) and reaching maximum ectoine and hydroxyectoine accumulation of 79 and 13 mg·gVSS^{-1}, respectively. Conversely, process operation at an EBRT of 27 min lead to microbial inhibition, resulting in a reduced biomass growth of 0.09 g·L·d^{-1} and an ectoine content of 47 mg·gVSS^{-1}. While the influence of diffuser pore size was less pronounced compared to EBRT, the optimal process performance was observed with a diffuser pore size of 0.6 mm.

1. Introduction

For decades, the biogas originated from the anaerobic digestion of organic waste and wastewaters has been massively employed as an energy vector via direct combustion in heat and power co-generation engines (EBA, 2022). Nevertheless, the rapid decrease of the production costs of competing renewable energies, especially solar and wind power, coupled to the prolonged instability in the local and global energy markets, have opened the door to the deployment of more innovative biogas valorization pathways (IRENA, 2023). Currently, the use of biogas as a source of green natural gas via upgrading, considered as strategic and intensively promoted by the European Commission, is leading the transition towards smarter uses of biogas (European Commission, 2022; Muñoz et al., 2015). Notwithstanding, as depicted in the "Innovating for sustainable growth" report, the valorization of biomass residues into energy or biofuels remains at the bottom of the added-value pyramid. The production of more sophisticated chemicals is mandatory for the future success of urban biorefineries, a crucial factor for achieving a more circular bioeconomy (European Commission, 2012, 2020).

In this context, the utilization of methanotrophic bacteria, capable of bioconverting the methane (CH_4) contained in the biogas in all sort of added-value products, has recently emerged as one of the most promising platforms for increasing biogas value (Pieja et al., 2017). Methanotrophs oxidize methane through a pathway that begins with methane conversion to methanol by methane monooxygenase (MMO). Methanol is then oxidized to formaldehyde by methanol dehydrogenase. Finally, formaldehyde is either assimilated for biomass growth or oxidized to CO_2 (Gęsicka et al., 2021). A significant variety of methanotrophs has demonstrated its ability to convert efficiently the CH_4 into bulk chemicals (polyhydroxyalkanoates (PHA)), feed and food products (single cell protein) or fine chemicals (ectoine) (Cantera et al., 2018a; García Martínez et al., 2022; Rodríguez et al., 2020). Particularly, the production of compatible solutes such as ectoine and hydroxyectoine, has attracted the attention of the cosmetic and pharmaceutical industries, given the high cost (1000 €·kg^{-1}) and low sustainability of their current

* Corresponding author. Institute of Sustainable Processes, University of Valladolid, 47011, Valladolid, Spain.
E-mail address: raul.munoz.torre@uva.es (R. Muñoz).

https://doi.org/10.1016/j.jenvman.2024.121811
Received 22 April 2024; Received in revised form 26 June 2024; Accepted 7 July 2024
Available online 14 July 2024

production processes, derived from the use of expensive carbon sources and complex downstream purification stages (Strong et al., 2015). Ectoine high market value relies on its high unparalleled performance as protein, cell membrane and tissue protector (Cantera et al., 2023). Ectoine synthesis occurs under high salinity conditions and begins with acetyl-CoA (produced via the serine pathway of CH_4 oxidation) and aspartate. This process involves three key enzymes encoded by the ectABC cluster: diaminobutyric acid aminotransferase (EctB), diaminobutyric acid acetyltransferase (EctA), and ectoine synthase (EctC) (Gęsicka et al., 2021). Ectoine can be converted into hydroxyectoine by the enzyme ectoine hydroxylase (EctD) (Bursy et al., 2007). Although ectoine and hydroxyectoine are produced intracellularly, they can be released into the medium in response to hypoosmotic shock when the salt concentration decreases (Rodero et al., 2023). The capacity of haloalkaliphilic methanotrophic cultures to simultaneously oxidize CH_4 and accumulate high contents of ectoine (70 mg ectoine·g^{-1} biomass) under saline stress conditions has been already optimized at lab scale (Carmona-Martínez et al., 2021; Rodero et al., 2022). Additionally, recent techno-economic and sensitivity studies have consistently demonstrated that ectoine production using haloalkaliphilic methanotrophic bacteria could significantly boost the economic revenue of small, medium and large waste treatment plants (Pérez et al., 2021).

However, the implementation of aerobic methanotrophy at industrial scale still faces some challenging biotechnological obstacles such as the low productivity of methanotrophic cultures due to the poor gas-liquid mass transfer efficiency of CH_4 and oxygen (Choi and Lee, 1999; Strong et al., 2016). The reduced gas-liquid mass transfer rates entail a concomitant increase of the gas empty bed residence time (EBRT) and incur in prohibited capital costs caused by the need of larger bioreactors (Pérez et al., 2022). The gas-liquid mass transfer rate is governed by the volumetric mass transfer coefficient K_{La} which relies, among other factors, on the hydrodynamics of the gas-liquid contact and on the morphology of these contactors. In spite of the successful advances in the design of innovative high-mass transfer bioreactors, such as Taylor flow, airlift or u-loop contactors and the development of operational strategies such as the internal gas recirculation or the use of pressurized bioreactors, some fundamental factors such as the gas diffusers morphology and the size of the membrane pores have not been carefully explored (Cattaneo et al., 2022; Garcia-Ochoa and Gomez, 2009; Stone et al., 2017). Therefore, an optimization of the bubble size in gas-liquid bioreactors becomes of paramount importance for reducing the capital and operational expenditures and concomitantly, boosting the economic performance of these novel bioprocesses.

The main goal of this work was the enhancement of the CH_4 bioconversion into ectoine and hydroxyectoine in bubble column bioreactors. The influence of the pore size of the membrane fine bubble gas diffusers was evaluated. Various gas EBRTs were tested to improve CH_4 mass transfer. Finally, specific ectoine and hydroxyectoine concentrations were analysed to determine the optimal operational conditions.

2. Materials and methods

2.1. Mineral salt medium and reagents

The mineral salt medium (MSM) had the following composition (per L of solution): 60 g NaCl, 3.78 g $NaHCO_3$, 3 g KNO_3, 0.2 g $MgSO_4{\cdot}7H_2O$, 0.11 g KH_2PO_4, 0.13 g $Na_2HPO_4{\cdot}2H_2O$, 0.013 g $CaCl_2{\cdot}2H_2O$, 0.07 mg $Na_2WO_2{\cdot}2H_2O$ and 2 mL of trace elements solution according to Carmona-Martínez et al. (2021). All chemicals (purity >99 %) were acquired from COFARCAS (Spain) and PanReac Applichem (Spain). A synthetic mixture of desulfurized biogas composed of 70 %v·v^{-1} CH_4 and 30 %v·v^{-1} CO_2 (Carburos Metalicos S.A.; Spain) was used in this study.

2.2. Experimental set-up

The experimental set-up was composed of two stand-alone PVC bubble column bioreactors (volume: 10 L, height: 67 cm, width: 10 cm, length: 20 cm) equipped with internal gas recirculation (Fig. 1). A custom-made diffuser consisting of a rubber membrane (12 cm × 5 cm) with a pore size of 0.3 or 0.6 mm was placed at the bottom of the bioreactors for gas supply. The inlet gas was composed of a mixture of synthetic biogas and air to provide a CH_4 concentration of 5 %v·v^{-1}. In order to prevent water condensation in the recirculation gas line, both bioreactors were interconnected to a condenser cooled at 10 °C prior recompression. An aliquot of 1 L·d^{-1} of exhausted culture medium without biomass was replaced by fresh MSM to limit the accumulation of inhibitory compounds and nutrient depletion according to Rodero et al. (2023), to provide a dilution rate of 0.1 d^{-1}. For this purpose, a 0.03 μm hollow fibre membrane module was installed inside the bioreactors to allow medium extraction without biomass loss. A biomass concentration of 3 g·L^{-1} in terms of volatile suspended solids (VSS) was maintained according to Rodero et al. (2022). In this context, a specific volume of the cultivation broth, determined by the measurements of VSS, was daily withdrawn and subjected to centrifugation (10,000 rpm, 10 min). The biomass-free cultivation broth was reinjected into the bioreactor while the bacterial biomass was discarded.

2.3. Operational procedures

The two bioreactors were operated in parallel in order to assess the influence of the diffuser pore size (0.3 and 0.6 mm) on the process performance. A methanotrophic bacterial consortium previously adapted to 6 %w·w^{-1} NaCl was used as inoculum in both bioreactors at an initial biomass concentration of 1.15 ± 0.07 g VSS·L^{-1}. The bacterial consortium was composed of the following main genera: *Methylomicrobium* (42 %), *Methylophaga* (15 %), *Nitratireductor* (10 %), *Lacimicrobium* (9%) and *Aequorivita* (5 %), among others (Rodero et al., 2022). Three different operational strategies were implemented to evaluate the influence of the gas EBRT on the CH_4 degradation and ectoine and hydroxyectoine synthesis by the methanotrophic consortium (Table 1). In stage 1, an inlet gas flowrate of 96 mL·min^{-1}, which corresponded to an EBRT of 104 min, was set. In stages 2 and 3 the inlet gas stream flowrates were increased up to 186 and 367 mL·min^{-1}, resulting in EBRTs of 54 and 27 min, respectively. These EBRTs were chosen because they were within the typical range of values applied for CH_4 removal in bubble column bioreactors (García-Pérez et al., 2018; Rodríguez et al., 2020). An internal gas recirculation of 7.0 ± 0.3·L min^{-1} in the bioreactors was maintained during the three operational stages. This internal gas recirculation flowrate was 73, 38 and 19 times higher than the inlet gas stream flowrate in stages 1, 2 and 3, respectively.

Gas samples of 100 μL from the inlet and outlet gas streams were withdrawn three times per week using gastight syringes to determine the CH_4 concentration. Gas flowrates at the inlet and outlet bioreactors streams were also monitored to accurately calculate CH_4 biodegradation. Inlet and outlet gas flow rates had different values due to the absorption and biological consumption of part of the inlet gas in the cultivation broth. Liquid samples of 200 mL from the cultivation broth were collected three times per week to determine pH, VSS concentration, and intra-cellular ectoine and hydroxyectoine concentration (i.e., the ectoine and hydroxyectoine that accumulate inside bacterial cells). No analysis of ectoine and hydroxyectoine in the cell-free cultivation broth (extra-cellular) was performed since, at high salinity, the amount of these osmolytes released into the medium is negligible (Cantera et al., 2017).

2.4. Analytical procedures

CH_4 concentration was determined using a Bruker 430 GC-TCD (Palo

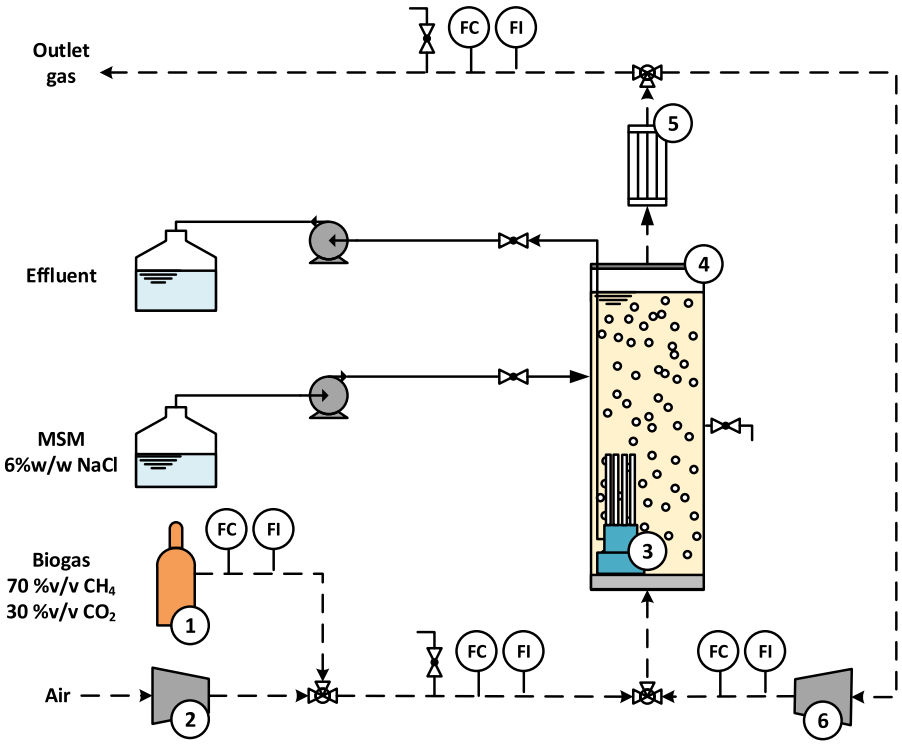

Fig. 1. Schematic diagram of the experimental set-up: (1) Biogas cylinder, (2) Air compressor, (3) Membrane module, (4) Bubble column bioreactor, (5) Condenser, (6) Recirculation compressor.

Table 1
Operational conditions tested during the optimization of biogas bioconversion into ectoines.

Operational stage	Reactor	Diffusor pore size (mm)	Methane loading rate ($g{\cdot}m^{-3}{\cdot}h^{-1}$)	EBRT (min)	Duration (d)
1	1	0.3	18	104	20
	2	0.6			
2	1	0.3	36	54	19
	2	0.6			
3	1	0.3	72	27	11
	2	0.6			

Alto, USA) equipped with a CP-Molsieve 5A and a CP-PoraBOND Q columns with helium as the carrier gas at 18 psi. The temperatures of the oven, injector and detector were maintained constant at 45, 150 and 200 °C, respectively. The inlet stream pressure was monitored with an Ifm Electronic pressure sensor (Germany) while the inlet and outlet gas flowrates were determined by means of the water displacement method. Biomass concentration, expressed as VSS concentration, was calculated according to standard methods (Eaton et al., 2005). A Hach Sension + PH3 pH meter (Düsseldorf, Germany) was used for pH measurements.

Intracellular ectoine and hydroxyectoine concentrations were determined by centrifuging 2 mL of culture broth at 9000×*g* for 10 min. After removing the supernatant, the pellet was washed with 6% $w{\cdot}w^{-1}$ NaCl solution prepared in Milli-Q water. Subsequently, 1.8 mL of 70% $v{\cdot}v^{-1}$ ethanol and approximately 25 ± 5 mg of 0.1 mm zirconia/silica beads (BioSpec, Spain) were added. The bacterial cells were lysed using a Mini-BeadBeater-16 at 1048×*g* for 10 min. The mixture was centrifuged again at 9000×*g* for 15 min and filtered through 0.22 μm filters for analysis. Finally, ectoines determination was performed via HPLC-UV (Cantera et al., 2020). The quantification of both compounds was performed using standards of ectoine and hydroxyectoine (purity ≥95 %, Sigma Aldrich) dissolved in ethanol at 70 $\%v{\cdot}v^{-1}$.

2.5. Data treatment

EBRT during each operational stage was calculated as:

$$EBRT = \frac{V}{Q_{in}} \quad (1)$$

where V represents the working liquid volume of the bioreactors (m^3) and Q_{in} the inlet gas flowrate ($m^3{\cdot}h^{-1}$).

CH_4 consumption was monitored by means of the CH_4 removal efficiency (CH_4-RE) and CH_4 elimination capacity (CH_4-EC), which were calculated according to equations (2) and (3):

$$CH_4 - RE = \frac{Q_{in}{\cdot}C_{CH_4,in} - Q_{out}{\cdot}C_{CH_4,out}}{Q_{in}{\cdot}C_{CH_4,in}} \quad (2)$$

$$CH_4 - EC = \frac{Q_{in}{\cdot}C_{CH_4,in} - Q_{out}{\cdot}C_{CH_4,out}}{V} \quad (3)$$

where Q_{out} is the outlet gas flowrate ($m^3{\cdot}h^{-1}$) and $C_{CH4,\mathrm{in}}$ and $C_{CH4,\mathrm{out}}$ stand for the inlet and outlet CH_4 mass concentration (g $CH_4{\cdot}m^{-3}$).

The intra-cellular concentrations of ectoine and hydroxyectoine ($mg_{ectoine/hydroxyectoine}{\cdot}g^{-1}_{biomass}$) were estimated using the biomass concentration (g $VSS{\cdot}L^{-1}$) in the bioreactors.

The results here presented were calculated as average values of the last 4 sampling points during each steady state, along with their corresponding standard deviations. VSS were provided as the average values together with their standard deviation based on duplicate technical measurements. T-student tests were conducted to assess the impact of the diffuser pore size on CH_4 removal and ectoine and hydroxyectoine production during the three operational stages. Additionally, one-way ANOVAs were performed to determine the influence of the EBRT under the different diffuser pore sizes tested.

3. Results and discussion

3.1. Influence of the membrane diffuser pore size and the EBRT on CH_4 removal

CH_4-RE and CH_4-EC are a function of the gas-liquid mass transfer in the bioreactor, which itself depends on design and operational parameters, such as the diffuser pore size or the EBRT. During stage 1, operation at an EBRT of 104 min and diffuser pore sizes of 0.3 and 0.6 mm in the bubble column bioreactors resulted in CH_4-REs of 56.5 ± 2.0 and 65.5 ± 2.4 %, respectively (Fig. 2A). These removal efficiencies corresponded to CH_4-ECs of 10.4 ± 0.5 and 11.8 ± 0.8 $g{\cdot}m^{-3}{\cdot}h^{-1}$, at 0.3 and 0.6 mm of pore size, respectively (Fig. 2B). Although typically, the decrease in diffuser pore size entails a concomitant decrease on the bubble size and, consequently, a higher gas-liquid contact area, the reduction in the pore size in the bubble column did not result in a higher CH_4 biodegradation performance. Indeed, the 2-fold decrease in the diffuser pore size exerted a negative impact on the CH_4 elimination under these operating conditions. These lower CH_4-REs achieved with a diffuser pore size of 0.3 mm could be attributed to the formation of pulse jets in the 0.3 mm pores, which resulted in lower gas-liquid interfacial areas and a poor mixing of the liquid phase in the bioreactor (Merchuk et al., 1998).

In stage 2, CH_4-REs of 62.5 ± 2.0 and 72.2 ± 1.2 % were recorded at EBRTs of 54 min and diffuser pore sizes of 0.3 and 0.6 mm, respectively. The decrease in EBRT to 54 min did not hinder the effective removal of CH_4. The higher CH_4-REs and higher inlet gas flowrates applied during this operational stage in comparison with stage 1 entailed an increase in CH_4-ECs (20.9 ± 1.0 and 23.9 ± 0.5 $g{\cdot}m^{-3}{\cdot}h^{-1}$, at 0.3 and 0.6 mm of pore size, respectively). The best process performance in terms of CH_4 removal was observed with the highest diffuser pore size, as recorded in stage 1. In this context, Gul et al. (2023) observed that a diffuser pore size of 1.5 mm resulted in more turbulent regime in comparison with that of 0.5 mm. When a turbulent flow is generated due to an intense mixing, the shear forces resulted in bubble break into smaller ones, increasing gas-liquid contact (Villadsen et al., 2011). Similarly, Bassani et al. (2017) reported a higher H_2 gas-liquid mass transfer using a diffuser with a pore size of 2 μm in comparison with that of 0.4 μm.

During stage 3, CH_4-REs of 63.4 ± 3.0 and 65.5 ± 1.7 %, which corresponded to CH_4-ECs of 43.9 ± 2.6 and 43.9 ± 2.2 $g{\cdot}m^{-3}{\cdot}h^{-1}$, were recorded in the bioreactors constructed with 0.3 and 0.6 mm of diffuser pore size, respectively (Fig. 2). In this stage, no influence of the diffuser pore size was observed. At the high flow rates sparged in phase 3, the formation of pulse jets in both 0.3 and 0.6 mm pore size membranes was likely similar, which resulted in similar CH_4-EC. No influence of EBRT between 27 and 54 min on CH_4-REs was observed using a diffuser pore size of 0.3 mm. However, CH_4-REs slightly decreased with the increment of the gas flowrate in the case of a diffuser pore size of 0.6 mm, which was attributed to a pernicious impact in the microbial activity (see section 3.2). Under both diffuser pore sizes, CH_4-ECs in stage 3 were two times higher than in stage 2 due to the nearly doubled inlet gas flow rate and similar CH_4-REs. Likewise, Rodríguez et al. (2020) reported an increase in the CH_4-EC from 41 to 74 $g{\cdot}m^{-3}{\cdot}h^{-1}$ with the decrease in the EBRT from 60 min to 30 min using a gas recirculation of 30 times the inlet gas recirculation and an inlet CH_4 concentration of 14 $\%v{\cdot}v^{-1}$. In comparison with the aforementioned study, the lower CH_4-ECs here obtained under similar EBRT (27 min) were mainly as a result of the use of lower concentrations of CH_4 in the inlet gas (5 $\%v{\cdot}v^{-1}$). Indeed, the increase in CH_4-ECs with the increase of the inlet CH_4 concentration was previously demonstrated (Rodero et al., 2022).

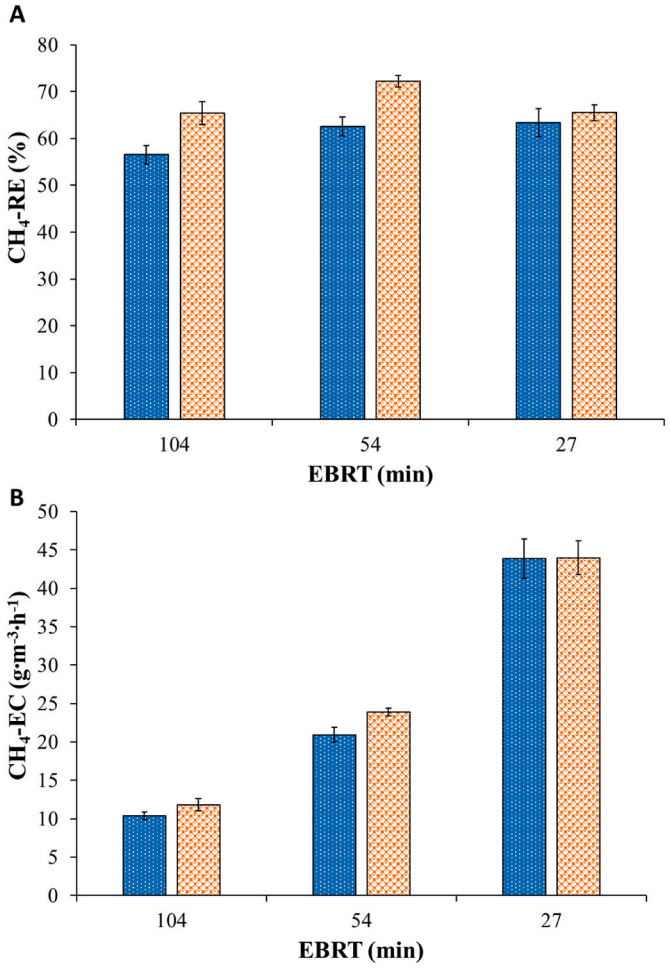

Fig. 2. Influence of the diffuser pore size (blue bars: 0.3 mm, orange bars: 0.6 mm) and the empty bed residence time (EBRT) on (A) methane removal efficiency and (B) methane elimination capacity. (For interpretation of the references to colour in this figure legend, the reader is referred to the Web version of this article.)

3.2. Influence of the diffuser pore size and the EBRT on biomass growth

The low gas inlet flowrate of 96 $mL{\cdot}min^{-1}$, and consequently, low methane inlet loading rate (18 $g{\cdot}m^{-3}{\cdot}h^{-1}$), together with the inherently low aqueous solubility of CH_4, resulted in a limitation of CH_4 bioavailability in stage 1. As a result, a poor biomass growth was observed under these conditions regardless of the diffuser pore size. A biomass concentration of 1.16 ± 0.12 g $VSS{\cdot}L^{-1}$ and 1.21 ± 0.34 g $VSS{\cdot}L^{-1}$ at 0.3 and 0.6 mm of diffuser pore size, respectively, were recorded along this operational stage, similar to the initial biomass concentration (Fig. 3). In stage 2, the increase in the methane loading rate up to 36 $g{\cdot}m^{-3}{\cdot}h^{-1}$ mediated a noticeable biomass growth, exceeding 3 g $VSS{\cdot}L^{-1}$ in both bioreactors. The increase in biomass during stage 2 confirmed that the limiting factor for microbial growth was the availability of CH_4. Consistently with higher CH_4-REs, biomass concentration was slightly higher when employing a diffuser pore size of 0.6 mm. In this regard, an average biomass productivity of 0.08 $g{\cdot}L{\cdot}d^{-1}$ and 0.17 $g{\cdot}L{\cdot}d^{-1}$ were obtained in the bioreactors with a diffuser pore size of 0.3 and 0.6 mm, respectively, during stage 2. The higher biomass production in the bioreactor operated with a diffuser pore size of 0.6 mm in comparison with that of 0.3 mm agreed with the higher CH_4-RE, and consequently, CH_4 consumption by methanotrophs.

The increase in gas flowrate up to 367 $mL{\cdot}min^{-1}$ in stage 3 did not impact positively on biomass growth, mainly in the bioreactor with a diffuser pore size of 0.6 mm. On the contrary, the biomass productivity in stage 3 decreased down to 0.07 $g{\cdot}L{\cdot}d^{-1}$ and 0.09 $g{\cdot}L{\cdot}d^{-1}$ in the bioreactors operated with a diffuser pore size of 0.3 and 0.6 mm, respectively. It has been previously reported in literature that inhibitory secondary metabolites, such as formate, methanol and nitrite, can be

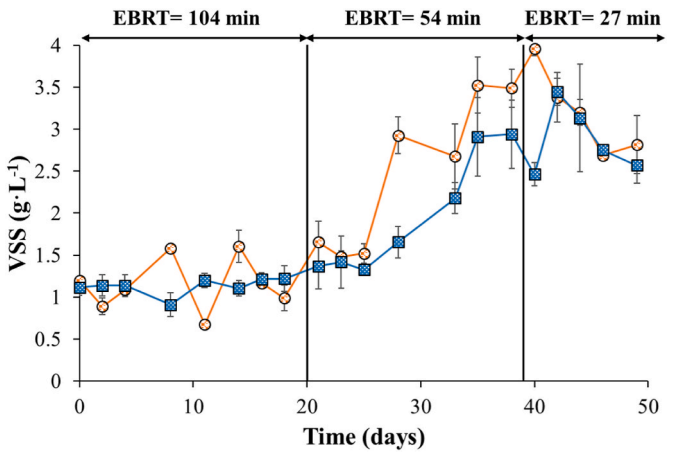

Fig. 3. Time course of biomass concentration as a function of the empty bed residence time in the bioreactor operated with a 0.3 mm (blue squares) and 0.6 mm (orange circles) pore size diffuser. (For interpretation of the references to colour in this figure legend, the reader is referred to the Web version of this article.)

excreted into the medium during CH_4 biodegradation in methanotrophic cultures at high methane loading rates (Cattaneo et al., 2022; Salem et al., 2021). In this regard, Cantera et al. (2020) demonstrated that the accumulation of toxic compounds could impact negatively the process efficiency in terms of CH_4-EC and ectoine accumulation. The increase in medium dilution rate favour the removal of these inhibitory compounds. Although part of the biomass-free broth was removed and replaced with fresh mineral salt medium, the higher CH_4 degradation in this stage as a result of the higher methane loading rate (72 $g{\cdot}m^{-3}{\cdot}h^{-1}$), could have induced a superior accumulation of these toxic byproducts.

3.3. *Influence of the diffuser pore size and the EBRT on ectoine and hydroxyectoine production*

A negligible impact ($p \geq 0.05$) of the diffuser pore size on ectoine biosynthesis was observed during the 3 operational stages (Fig. 4A). During operation under an EBRT of 104 min, specific ectoine concentrations of 68 ± 11 and 69 ± 15 $mg{\cdot}gVSS^{-1}$ were recorded using a diffuser pore size of 0.3 and 0.6 mm, respectively. Similar specific ectoine concentrations (74 ± 11 $mg{\cdot}gVSS^{-1}$ and 79 ± 11 $mg{\cdot}gVSS^{-1}$ in bioreactor 1 and 2, respectively) were also obtained regardless of diffuser pore size at stage 2. Thus, the decrease in EBRT from 104 min to 54 min, which implied a higher CH_4 gas-liquid transfer and a consistently active biomass growth, did not result in a significant increase on specific ectoine concentrations. The higher biomass productivity in stage 2 in comparison with stage 1, resulted in ectoine productivities of 6–13 $mg{\cdot}L^{-1}{\cdot}d^{-1}$, 8 times higher than those of stage 1. Interestingly, the decrease in EBRT to 27 min during stage 3 did not result in an increase in the specific ectoine content. Indeed, a significant decrease in ectoine concentrations down to 45 ± 4 $mg{\cdot}gVSS^{-1}$ and 47 ± 14 $mg{\cdot}gVSS^{-1}$ were recorded in this stage in the bioreactors operated with a diffuser pore size of 0.3 and 0.6 mm, respectively. This decrease in ectoine biosynthesis, which matched the deterioration in biomass growth, was attributed to the accumulation of toxic metabolites caused by the low dilution rate applied (0.1 d^{-1}) and the high methane loading rate (72 g m^{-3} h^{-1}). The specific ectoine concentrations obtained in this study (45–79 $mg{\cdot}gVSS^{-1}$) were within the range of those reported in previous studies (27–94 mg ectoine$\cdot gVSS^{-1}$) by pure or mixed cultures of methanotrophs (Cantera et al., 2018b; Rodero et al., 2023). However, these yields were lower than those typically obtained by *Halomonas* sp. using glucose or glutamate as a carbon source (Table 2). The maximum ectoine productivity here achieved (13 $mg{\cdot}L^{-1}{\cdot}d^{-1}$) was superior than the highest productivity reported by Cantera et al. (2020) (10 $mg{\cdot}L^{-1}{\cdot}d^{-1}$) using a haloalkaliphilic methanotrophic consortium fed with biogas in a bubble column bioreactor.

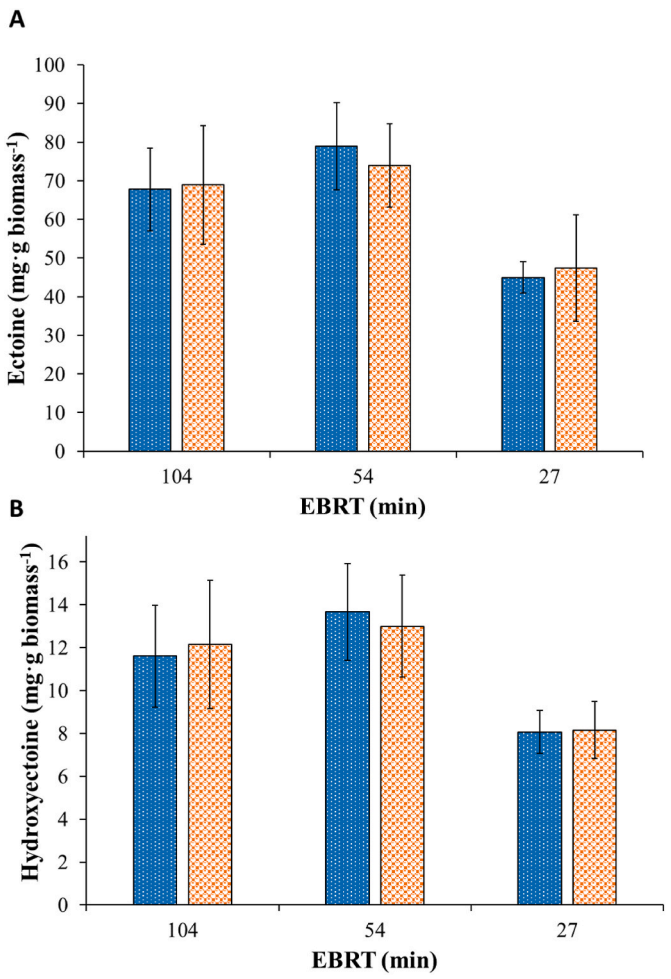

Fig. 4. Influence of the diffuser pore size (blue bars: 0.3 mm, orange bars: 0.6 mm) and the empty bed residence time (EBRT) on (A) ectoine accumulation and (B) hydroxyectoine accumulation. (For interpretation of the references to colour in this figure legend, the reader is referred to the Web version of this article.)

Table 2
Ectoine and hydroxyectoine production by different microorganisms.

Strain	Yields ($g{\cdot}g_{VSS}$)		Reference
	Ectoine	Hydroxyectoine	
Halomonas elongata	0.11	–	Sauer and Galinski (1998)
Halomonas salina	0.14	–	Lang et al. (2011)
Brevibacterium epidermis	0.05	–	Onraedt et al. (2005)
Hansenula polymorpha	–	0.058	Eilert et al. (2013)
Methylomicrobium alcaliphilum 20Z	0.11	–	Cantera et al. (2020)
Enriched haloalkaliphilic consortium	0.057	0.051	Carmona-Martínez et al. (2021)
Enriched haloalkaliphilic consortium	0.079	0.013	In this work

Similarly, no influence ($p \geq 0.05$) of the diffuser pore size in hydroxyectoine bacterial content was observed regardless of the EBRT tested (Fig. 4B). A specific hydroxyectoine concentration of 12 ± 3 $mg{\cdot}gVSS^{-1}$ was achieved at an EBRT of 104 min regardless of the diffuser pore size. A negligible impact ($p \geq 0.05$) on the specific hydroxyectoine content (13 ± 2 $mg{\cdot}gVSS^{-1}$) was also recorded with the

decrease in EBRT to 54 min during stage 2. However, the maximum hydroxyectoine productivity was obtained in this stage as a result of superior biomass growth in comparison to stage 1 (1–2 mg·L^{-1}·d^{-1}). The lower biomass growth and ectoine biosynthesis at an EBRT of 27 min was also correlated with hydroxyectoine accumulation by methanotrophs. Indeed, specific hydroxyectoine concentrations of 8 ± 1 mg·$gVSS^{-1}$ were recorded in stage 3 in both bioreactors. Hydroxyectoine production was 4–6 folds lower than ectoine production and similar that in previous studies (ectoine biosynthesis 3–7 folds higher than hydroxyectoine synthesis) (Rodero et al., 2022, 2023). The reason is that hydroxyectoine production requires the conversion of ectoine via a stereospecific hydroxylation (Bursy et al., 2007). Nevertheless, the highest specific hydroxyectoine concentrations attained in this study were lower compared to those reported using a consortium enriched from a salt lagoon growing at 9 %w·w^{-1} NaCl (51 mg hydroxyectoine·$gVSS^{-1}$), a pure culture of *Hansenula polymorpha* (58 mg hydroxyectoine·$gVSS^{-1}$), or an engineered *M. alcaliphilum 20Z* (22 mg hydroxyectoine·$gVSS^{-1}$) (Carmona-Martínez et al., 2021; Eilert et al., 2013; Mustakhimov et al., 2019).

Despite the promising results observed in the production of ectoine from air-diluted biogas, several limitations need to be addressed. While this study improved CH_4 gas-liquid mass transfer, the efficiency of CH_4 fixation by methanotrophs requires further optimization. Specific growth rates and yields of ectoine and hydroxyectoine require enhancement. The stability of the methanotroph consortium has not been studied and could potentially impact long-term production. Finally, the scalability of the process was not addressed.

4. Conclusions

The results of this study provide new insights into the optimal operating conditions to improve biogas ectoine and hydroxectoine production. The EBRT has been shown to play a crucial role in process performance, primarily impacting the gas-liquid transfer of CH_4 and, subsequently, the availability of CH_4 for methanotrophic growth. Interestingly, the impact of the diffuser pore size within the tested range (0.3–0.6 mm) has been less significant. The optimal conditions for maximizing biomass growth, and consequently, ectoine and hydroxyectoine production, were determined to be an EBRT of 54 min and a diffuser pore size of 0.6 mm. Further research is needed to explore process optimization at pilot scale to allow a successful process optimization.

CRediT authorship contribution statement

María del Rosario Rodero: Writing – original draft, Visualization, Investigation, Formal analysis. **Víctor Pérez:** Writing – original draft, Visualization. **Raúl Muñoz:** Writing – review & editing, Supervision, Funding acquisition, Conceptualization.

Declaration of competing interest

The authors declare the following financial interests/personal relationships which may be considered as potential competing interests: Raul Munoz reports financial support was provided by European Union. Raul Munoz reports financial support was provided by Regional Government of Castilla y Leon. If there are other authors, they declare that they have no known competing financial interests or personal relationships that could have appeared to influence the work reported in this paper.

Data availability

Data will be made available on request.

Acknowledgements

This work was supported by the DEEP PURPLE project. This project has received funding from the Bio-based Industries Joint Undertaking (JU) under the European Union's Horizon 2020 research and innovation programme under the grant agreement N° 837998. The JU receives support from the European Union's Horizon 2020 research and innovation programme and the Bio-based Industries Consortium. This work was also supported by the Regional Government of Castilla y León and the EU-FEDER (CLU 2017-09, CL-EI-2021-07, UIC 315). María del Rosario Rodero acknowledges the NextGenerationEU Margarita Salas programme from the European Union for her research contract.

References

Bassani, I., Kougias, P.G., Treu, L., Porté, H., 2017. Optimization of hydrogen dispersion in thermophilic up-flow reactors for ex-situ biogas upgrading. Bioresour. Technol. https://doi.org/10.1016/j.biortech.2017.03.055.

Bursy, J., Pierik, A.J., Pica, N., Bremer, E., 2007. Osmotically induced synthesis of the compatible solute hydroxyectoine is mediated by an evolutionarily conserved ectoine hydroxylase. J. Biol. Chem. 282, 31147–31155. https://doi.org/10.1074/jbc.M704023200.

Cantera, S., Di Benedetto, F., Tumulero, B.F., Sousa, D.Z., 2023. Microbial conversion of carbon dioxide and hydrogen into the fine chemicals hydroxyectoine and ectoine. Bioresour. Technol. 374, 128753 https://doi.org/10.1016/j.biortech.2023.128753.

Cantera, S., Lebrero, R., Rodríguez, S., García-Encina, P.A., Muñoz, R., 2017. Ectoine bio-milking in methanotrophs: a step further towards methane-based bio-refineries into high added-value products. Chem. Eng. J. 328, 44–48. https://doi.org/10.1016/j.cej.2017.07.027.

Cantera, S., Muñoz, R., Lebrero, R., López, J.C., Rodríguez, Y., García-Encina, P.A., 2018a. Technologies for the bioconversion of methane into more valuable products. Curr. Opin. Biotechnol. 50, 128–135. https://doi.org/10.1016/j.copbio.2017.12.021.

Cantera, S., Phandanouvong-Lozano, V., Pascual, C., García-Encina, P.A., Lebrero, R., Hay, A., Muñoz, R., 2020. A systematic comparison of ectoine production from upgraded biogas using Methylomicrobium alcaliphilum and a mixed haloalkaliphilic consortium. Waste Manag. 102, 773–781. https://doi.org/10.1016/j.wasman.2019.11.043.

Cantera, S., Sánchez-Andrea, I., Lebrero, R., García-Encina, P.A., Stams, A.J.M., Muñoz, R., 2018b. Multi-production of high added market value metabolites from diluted methane emissions via methanotrophic extremophiles. Bioresour. Technol. 267, 401–407. https://doi.org/10.1016/j.biortech.2018.07.057.

Carmona-Martínez, A.A., Marcos-Rodrigo, E., Bordel, S., Marín, D., Herrero-Lobo, R., García-Encina, P.A., Muñoz, R., 2021. Elucidating the key environmental parameters during the production of ectoines from biogas by mixed methanotrophic consortia. J. Environ. Manag. 298 https://doi.org/10.1016/j.jenvman.2021.113462.

Cattaneo, C.R., Rodríguez, Y., Rene, E.R., García-Depraect, O., Muñoz, R., 2022. Biogas bioconversion into poly(3-hydroxybutyrate) by a mixed microbial culture in a novel Taylor flow bioreactor. Waste Manag. 150, 364–372. https://doi.org/10.1016/j.wasman.2022.07.017.

Choi, J., Lee, S.Y., 1999. Factors affecting the economics of polyhydroxyalkanoate production by bacterial fermentation. Appl. Microbiol. Biotechnol. 51, 13–21. https://doi.org/10.1007/s002530051357.

Eaton, M.A.H., Clesceri, A.D., Rice, L.S., Greenberg, E.W., Franson, A.E., 2005. APHA: Standard Methods for the Examination of Water and Wastewater, Centen. ed. APHA, AWWA, WEF, Washington, DC.

EBA, 2022. European Biogas Association. Statistical Report 2022. Tracking biogas and biomethane deployment across Europe, Brussels.

Eilert, E., Kranz, A., Hollenberg, C.P., Piontek, M., Suckow, M., 2013. Synthesis and release of the bacterial compatible solute 5-hydroxyectoine in Hansenula polymorpha. J. Biotechnol. 167, 85–93. https://doi.org/10.1016/j.jbiotec.2013.02.005.

European Comission, 2022. REPowerEU Plan. Brussels.

European Commission, 2020. A New Circular Economy Action Plan for a Cleaner and More Competitive Europe. European Comission, Luxembourg. https://doi.org/10.2779/05068.

European Commission, 2012. Innovating for sustainable growth: a bioeconomy for Europe. Off. J. Eur. Union 64. https://doi.org/10.2777/6462.

Garcia-Ochoa, F., Gomez, E., 2009. Bioreactor scale-up and oxygen transfer rate in microbial processes: an overview. Biotechnol. Adv. 27, 153–176. https://doi.org/10.1016/j.biotechadv.2008.10.006.

García-Pérez, T., López, J.C., Passos, F., Lebrero, R., Revah, S., Muñoz, R., 2018. Simultaneous methane abatement and PHB production by Methylocystis hirsuta in a novel gas-recycling bubble column bioreactor. Chem. Eng. J. 334, 691–697. https://doi.org/10.1016/j.cej.2017.10.106.

García Martínez, J.B., Pearce, J.M., Throup, J., Cates, J., Lackner, M., Denkenberger, D. C., 2022. Methane single cell protein: potential to secure a global protein supply against catastrophic food shocks. Front. Bioeng. Biotechnol. 10, 1–18. https://doi.org/10.3389/fbioe.2022.906704.

Gęsicka, A., Oleskowicz-Popiel, P., Łężyk, M., 2021. Recent trends in methane to bioproduct conversion by methanotrophs. Biotechnol. Adv. 53, 107861 https://doi.org/10.1016/j.biotechadv.2021.107861.

Gul, A., Derakhshandeh, M., Un, U.T., 2023. Optimization of carbon dioxide absorption in a continuous bubble column reactor using response surface methodology. Environ. Qual. Manag. 33, 79–93. https://doi.org/10.1002/tqem.22020.

IRENA, 2023. International renewable energy agency. Renewable energy statistics 2023, Abu Dhabi. https://www.irena.org/-/media/Files/IRENA/Agency/Publication/2023/Jul/IRENA_Renewable_energy_statistics_2023.pdf?rev=7b2f44c294b84cad9a27fc24949d2134.

Lang, Y., Bai, L., Ren, Y., Zhang, L., Nagata, S., 2011. Production of ectoine through a combined process that uses both growing and resting cells of Halomonas salina DSM 5928T. Extremophiles 15, 303–310. https://doi.org/10.1007/s00792-011-0360-9.

Merchuk, J.C., Contreras, A., García, F., Molina, E., 1998. Studies of mixing in a concentric tube airlift bioreactor with different spargers. Chem. Eng. Sci. 53, 709–719. https://doi.org/10.1016/S0009-2509(97)00340-0.

Muñoz, R., Meier, L., Diaz, I., Jeison, D., 2015. A review on the state-of-the-art of physical/chemical and biological technologies for biogas upgrading. Rev. Environ. Sci. Biotechnol. 14, 727–759. https://doi.org/10.1007/s11157-015-9379-1.

Mustakhimov, I.I., Reshetnikov, A.S., But, S.Y., Rozova, O.N., Khmelenina, V.N., Trotsenko, Y.A., 2019. Engineering of hydroxyectoine production based on the Methylomicrobium alcaliphilum. Appl. Biochem. Microbiol. 55, 626–630. https://doi.org/10.1134/S0003683819130015.

Onraedt, A.E., Walcarius, B.A., Soetaert, W.K., Vandamme, E.J., 2005. Optimization of ectoine synthesis through fed-batch fermentation of Brevibacterium epidermis. Biotechnol. Prog. 21, 1206–1212. https://doi.org/10.1021/bp0500967.

Pérez, V., Moltó, J.L., Lebrero, R., Muñoz, R., 2022. Ectoine production from biogas: a sensitivity analysis. Effect of local commodity prices, economy of scale, market trends and biotechnological limitations. J. Clean. Prod. 369 https://doi.org/10.1016/j.jclepro.2022.133440.

Pérez, V., Moltó, J.L., Lebrero, R., Muñoz, R., 2021. Ectoine production from biogas in waste treatment facilities: a techno-economic and sensitivity analysis. ACS Sustain. Chem. Eng. https://doi.org/10.1021/acssuschemeng.1c06772.

Pieja, A.J., Morse, M.C., Cal, A.J., 2017. Methane to bioproducts: the future of the bioeconomy? Curr. Opin. Chem. Biol. 41, 123–131. https://doi.org/10.1016/j.cbpa.2017.10.024.

Rodero, M. del R., Carmona-Martínez, A.A., Martínez-Fraile, C., Herrero-Lobo, R., Rodríguez, E., García-Encina, P.A., Peña, M., Muñoz, R., 2023. Ectoines production from biogas in pilot bubble column bioreactors and their subsequent extraction via bio-milking. Water Res. 245, 120665 https://doi.org/10.1016/j.watres.2023.120665.

Rodero, M. del R., Herrero-Lobo, R., Pérez, V., Muñoz, R., 2022. Influence of operational conditions on the performance of biogas bioconversion into ectoines in pilot bubble column bioreactors. Bioresour. Technol. 358 https://doi.org/10.1016/j.biortech.2022.127398.

Rodríguez, Y., Firmino, P.I.M., Pérez, V., Lebrero, R., Muñoz, R., 2020. Biogas valorization via continuous polyhydroxybutyrate production by Methylocystis hirsuta in a bubble column bioreactor. Waste Manag. 113, 395–403. https://doi.org/10.1016/j.wasman.2020.06.009.

Salem, R., Soliman, M., Fergala, A., Audette, G.F., ElDyasti, A., 2021. Screening for methane utilizing mixed communities with high polyhydroxybutyrate (PHB) production capacity using different design approaches. Polymers 13. https://doi.org/10.3390/polym13101579.

Sauer, T., Galinski, E.A., 1998. Bacterial milking: a novel bioprocess for production of compatible solutes. Biotechnol. Bioeng. 57, 306–313. https://doi.org/10.1002/(SICI)1097-0290(19980205)57:3<306::AID-BIT7>3.0.CO;2-L.

Stone, K.A., Hilliard, M.V., He, Q.P., Wang, J., 2017. A mini review on bioreactor configurations and gas transfer enhancements for biochemical methane conversion. Biochem. Eng. J. 128, 83–92. https://doi.org/10.1016/j.bej.2017.09.003.

Strong, P.J., Kalyuzhnaya, M., Silverman, J., Clarke, W.P., 2016. A methanotroph-based biorefinery: potential scenarios for generating multiple products from a single fermentation. Bioresour. Technol. 215, 314–323. https://doi.org/10.1016/j.biortech.2016.04.099.

Strong, P.J., Xie, S., Clarke, W.P., 2015. Methane as a resource: can the methanotrophs add value? Environ. Sci. Technol. 49, 4001–4018. https://doi.org/10.1021/es504242n.

Villadsen, J., Nielsen, J., Lidén, G., 2011. Principles, Bioreaction Engineering.